Photothermocatalytic Synergetic Effect Leads to High Efficient Detoxification of Benzene on TiO2 and Pt/TiO2 Nanocomposite

ARTICLE *in* CHEMCATCHEM · SEPTEMBER 2010

Impact Factor: 4.56 · DOI: 10.1002/cctc.201000085

5 AUTHORS, INCLUDING:

Yuanzhi Li
Wuhan University of Technology
60 PUBLICATIONS **1,953** CITATIONS

SEE PROFILE

Jie Xu
University of South Australia
12 PUBLICATIONS **141** CITATIONS

SEE PROFILE

Xiujian Zhao
Wuhan University of Technology
456 PUBLICATIONS **7,216** CITATIONS

SEE PROFILE

DOI: 10.1002/cctc.201000085

Photothermocatalytic Synergetic Effect Leads to High Efficient Detoxification of Benzene on TiO_2 and Pt/TiO_2 Nanocomposite

Yuanzhi Li,* Jichao Huang, Tao Peng, Jie Xu, and Xiujian Zhao[a]

Controlling the emission of volatile organic compound (VOCs) has become an important issue because they are not only hazardous to human health but also harmful to the environment.[1] Among various VOCs, the carcinogenic and recalcitrant benzene, which is one of the most abundant aromatic hydrocarbons found in polluted urban atmospheres, has been regarded as a priority hazardous substance for which efficient treatment technologies are needed.[2] Heterogeneous photocatalysis based on nanostructured TiO_2 has attracted much research attention in the past decades as an important and promising technology for the detoxification of organic pollutants because of the superior photocatalytic activity, chemical stability, low cost, and nontoxicity of TiO_2. However, when TiO_2 photocatalysts are applied to the detoxification of benzene in the gas phase, they are prone to deactivation mainly due to the deposition of less reactive byproducts on the TiO_2 surface, making the photocatalytic detoxification of benzene very inefficient.[3,4] Much effort has therefore been devoted to enhancing the efficiency of benzene photocatalytic oxidation. The modification of TiO_2 with noble metal (e.g., Rh and Pt) as co-catalysts has been found to boost the efficiency of benzene photocatalytic oxidation and improve the durability of TiO_2 catalysts.[5–7] Recently, photocatalytic oxidation combined with ozone oxidation on TiO_2 has been developed to improve the efficiency of benzene or toluene oxidation.[8,9] As ozone is also an air pollutant, additional setup was required to remove the its excess. Plasma-driven photocatalysis and catalysis have been reported to enhance VOC decomposition activity on TiO_2 and Al_2O_3.[10] Developing a highly efficient and cost-effective strategy for the detoxification of recalcitrant VOCs, such as benzene, has been a great challenge. Herein, photocatalysis and thermal catalysis have been ideally combined together just by a facile method of coating TiO_2 catalyst and Pt/TiO_2 nanocomposite on the surfaces of a UV lamp without using any additional heater, by which both UV irradiation and nonradiative thermal energy emitted from the UV lamp are fully used, and the high efficient photothermocatalytic detoxification of benzene has been realized. In this perfect combination of photocatalysis and thermal catalysis, a new photothermocatalytic synergetic effect has been found for the first time.

Various high-pressure Hg lamps have been widely used as UV light sources in photocatalytic studies for decades. However, their nonradiative thermal energy emitted has not been fully used. In the closed gas-phase reactor, when the self-rectified high-pressure Hg lamp was turned on, the thermal energy emitted from the lamp made its surface temperature automatically increase to 240 °C, which provided a possibility for photothermocatalytic oxidation to occur without using an additional heater. The TiO_2 sample was coated on the surfaces of the lamp, and thus the TiO_2 catalyst was co-excited by both UV irradiation and thermal energy. Under the photothermocatalytic condition, benzene was rapidly oxidized with time and

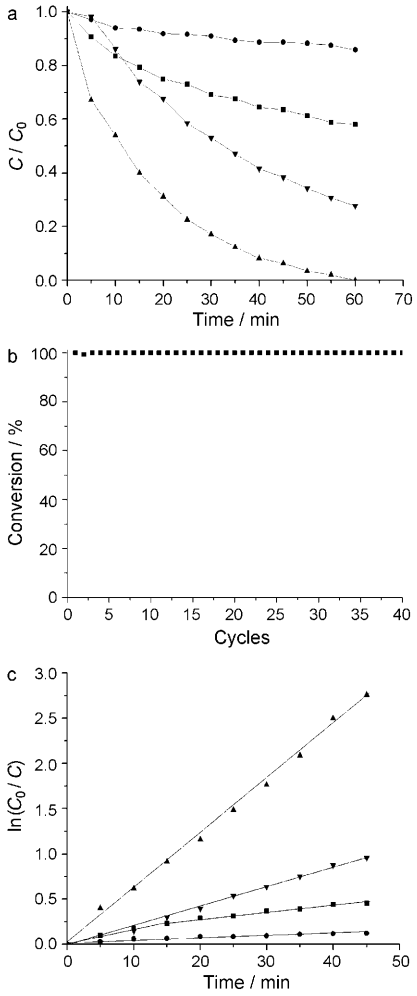

Figure 1. a) The time course of the decrease in benzene concentration and c) $\ln(C_0/C)$ on the TiO_2 catalyst under different conditions: Photothermocatalytic oxidation with UV irradiation at 240 °C (▲), photocatalytic oxidation with UV irradiation at 40 °C (■), thermocatalytic oxidation at 240 °C (●), photocatalytic oxidation at 40 °C under the UV irradiation energy or photons absorbed by the TiO_2 catalyst identical to that in the case of the photothermocatalytic oxidation at 240 °C (▼); b) the durability of the TiO_2 catalyst for the photothermocatalytic oxidation of benzene.

[a] *Prof. Y. Li, Prof. J. Huang, T. Peng, J. Xu, X. Zhao*
Key Laboratory of Silicate Materials Science and Engineering
Wuhan University of Technology
Ministry of Education, 122 Luoshi Road, Wuhan 430070 (China)
Fax: (+86) 27-87883743
E-mail: liyuanzhi66@hotmail.com

Supporting information for this article is available on the WWW under http://dx.doi.org/10.1002/cctc.201000085.

accompanied with the production of a large amount of CO_2 (Figure 1a). No organic products were detected by GC. After 60 min, benzene was completely oxidized, and the concentration of CO_2 produced was 473.5 mg m^{-3} (see the Supporting Information, Figure S1). The color of the TiO_2 catalyst remained unchanged after the photothermocatalytic oxidation. In contrast, benzene was slowly degraded under the thermocatalytic condition at the same temperature as the photothermocatalytic oxidation (240 °C). After 60 min, only 16.3% of benzene was degraded, and the concentration of CO_2 produced was 84.0 mg m^{-3}. The color of the TiO_2 catalyst changed from white to yellowish brown, which indicated that the carbon deposits were formed on the TiO_2 surface. Under the photocatalytic condition (40 °C), 48.4% of benzene was degraded, and the concentration of CO_2 produced was 64.8 mg m^{-3} after 60 min. The color of the TiO_2 catalyst changed from white to yellowish, which indicated that the carbon deposits were formed on the TiO_2 surface during the photocatalytic process.

The photocatalytic oxidation of aromatic compounds on TiO_2 experiences a quick deactivation due to the strong adsorption of the produced carbon deposits on TiO_2.[3,7] A similar phenomenon of catalyst deactivation after the photocatalytic oxidation occurred in our case because no CO_2 was detected after the TiO_2 catalyst had been recycled four times. The TiO_2 catalyst exhibited an excellent durability for the photothermocatalytic oxidation (Figure 1b). After the TiO_2 catalyst had been recycled 40 times, its photothermocatalytic activity remained unchanged. These results indicate that the photothermocatalytic oxidation on TiO_2 is a very efficient approach for the detoxification of benzene. The used TiO_2 catalysts after the test of benzene oxidation were characterized by FTIR. Carbon deposits were detected on the used TiO_2 catalysts after the tests of both photocatalytic and thermocatalytic oxidation, evidenced by the appearance of several peaks in the range of 1000–1150 cm^{-1}, which was assigned to C–O stretching (Figure S2).[11] In contrast, both the used TiO_2 catalyst after the test of the photothermocatalytic oxidation and the recycled TiO_2 catalyst exhibited FTIR spectra almost similar to that of the fresh TiO_2 catalyst. The recycled TiO_2 catalyst maintained a structural state similar to that of the fresh TiO_2 catalyst, which could explain its excellent durability for the photothermocatalytic oxidation.

The photocatalytic, thermocatalytic, and photothermocatalytic oxidation of benzene generally followed first-order kinetics (Figure 1c). The rate constant for the photothermocatalytic oxidation ($k_{ptc}=6.0\times10^{-2}$ min^{-1}) was 7.6 and 33.3 times higher than that for the photocatalytic oxidation ($k_{pc}=7.9\times10^{-3}$ min^{-1}) and that for the thermocatalytic oxidation ($k_{tc}=1.8\times10^{-3}$ min^{-1}), respectively.

The UV intensity on the surface of the UV lamp depends on the measurement position, and its average intensity was estimated to be 3976.7 μW cm^{-2}. The UV intensity on the bottom of the reactor, where the catalyst on a glass dish for the above photocatalytic or thermocatalytic oxidation was set, was 1282.2 μW cm^{-2}. Obviously, the UV irradiation energy or photons absorbed by the TiO_2 catalyst in the photothermocatalytic case was much larger than that in the photocatalytic case. To make a more accurate comparison between the photothermocatalytic and photocatalytic oxidation, the UV irradiation photons absorbed by the TiO_2 catalyst in both cases should be identical. TiO_2 powder (0.5000 g) was coated on the whole inner wall of the reactor, and thus all of the UV irradiation photons emitted from the UV lamp could be absorbed by the TiO_2 catalyst as in the case of directly coating the same amount of the TiO_2 catalyst on the surface of the UV lamp for the photothermocatalytic oxidation. Increasing the absorbed UV irradiation photons led to a considerable enhancement of the photocatalytic activity (Figure 1a). 72.2% of benzene was degraded after 60 min, and the concentration of CO_2 produced was 309.0 mg m^{-3}(see the Supporting Information, Figure S1). However, even under this photocatalytic condition, its rate constant ($k_{pc}=2.3\times10^{-2}$ min^{-1}) was still much lower than the photothermocatalytic rate constant (Figure 1c). In the case of the photothermocatalytic oxidation, if the photocatalytic oxidation in parallel with the thermocatalytic oxidation independently proceeds, that is, $dC/dt=k_{pc}C+k_{tc}C$, k_{ptc} should be equal to ($k_{pc}+k_{tc}$) (2.48×10^{-2} min^{-1}). However, k_{ptc} was 2.4 times higher than ($k_{pc}+k_{tc}$). Therefore, a synergetic effect between the photocatalytic and thermocatalytic oxidation did exist in the photothermocatalytic oxidation.

It has been reported that benzene adsorbed on TiO_2 at lower temperature (less than 200 K) desorbs with increasing temperature; above 300 K, complete desorption of benzene results.[12] In our experiment, we also did not observe the vibration mode of benzene (e.g., C–H stretching: 3000–3100 cm^{-1}, C=C stretching: 1580–1600 cm^{-1})[11] on the fresh TiO_2 (P25) catalyst by FTIR at room temperature. Therefore, the much higher photothermocatalytic activity at 240 °C compared to the photocatalytic activity at 40 °C originated from factors other than their difference in the adsorption amount of benzene on the TiO_2 catalyst at the different temperatures.

To investigate the origin of the synergetic effect, several experiments were designed as follows. As both photocatalytic and thermocatalytic oxidations of benzene probably simultaneously take place under the UV irradiation at 240 °C, it is difficult to independently evaluate the effect of temperature on the photocatalytic oxidation without thermocatalytic oxidation. It is widely accepted that the separation efficiency of photogenerated electrons and holes plays a decisive role in the photocatalytic reaction, and the photocurrent measurement is another way to measure the photocatalytic activity: the higher the photocurrent, the higher the separation efficiency, and thus, the higher the photocatalytic activity. Therefore, we investigated the effect of temperature on the photocurrent of a TiO_2 electrode in the absence of benzene. The TiO_2 electrode exhibited considerable photocurrent under the UV irradiation at 40 °C (Figure 2). Increasing the measurement temperature led to a quick decrease of the photocurrent, which was attributed to the decrease of the mobility of charge carrier in TiO_2 with increase in temperature, and the faster recombination rate of the photogenerated electrons and holes at higher temperature than that at lower temperature.[13] When the temperature increased to 240 °C, the photocurrent was quite low. The dramatic decrease in the photocurrent suggests that the photoca-

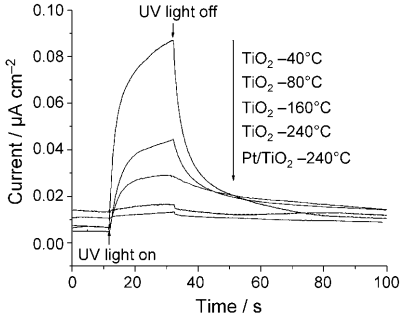

Figure 2. The transient response of the photocurrent for the TiO_2 and 0.1 wt% Pt/TiO_2 electrode in the absence of benzene under the UV irradiation at different temperatures.

talytic activity significantly decreased with increasing reaction temperature to 240 °C, which is in striking contrast to the above observation that the photothermocatalytic oxidation was much more efficient than the combination of both the photocatalytic and thermocatalytic oxidation. This result reveals that the synergetic effect probably originated from a novel mechanism of the photothermocatalytic oxidation.

It has been widely accepted that the thermocatalytic oxidation of hydrocarbon on metal oxide follows a mechanism called the Mars–van Krevelen redox cycle.[14,15] According to this mechanism, both gaseous and lattice oxygen play active roles in hydrocarbon oxidation. The hydrocarbon is first oxidized by the lattice oxygen in the oxide catalyst, and then the reduced oxide catalyst is reoxidized later by gaseous oxygen. Recent studies have reported that the activation of lattice oxygen from TiO_2 is the key step in the mechanism that drives the thermal decomposition of organic pollutants such as dimethyl methylphosphonate and 2-chloroethyl ethyl sulfide in the absence of gaseous oxygen.[16,17] Thus we investigated the effect of UV irradiation on the reaction between benzene and the lattice oxygen in TiO_2 in the absence of gaseous O_2. The concentration of CO_2 produced at 240 °C without UV irradiation increased to 35.9 mg m^{-3} after 75 min (Figure 3a). As there was no gaseous oxygen in the reactor, the oxygen in the produced CO_2 originated from the lattice oxygen in the TiO_2 catalyst. The X-ray photoelectron spectroscopy (XPS) results revealed that there were surface species of titanium suboxides TiO_x ($x<2$) in the used TiO_2 catalyst (Figure S3). These results indicated that benzene was oxidized to CO_2 by the lattice oxygen in TiO_2 accompanied by the formation of TiO_x. The X-ray diffraction (XRD) results indicated that the formation of TiO_x did not change its bulk crystalline structure (Figure S4). Interestingly, UV irradiation on the TiO_2 catalyst, of which the intensity was 1282.2 μW cm^{-2}, significantly increased the formation rate of CO_2 through the oxidation of benzene by the lattice oxygen in TiO_2 at 240 °C. The concentration of CO_2 produced at 240 °C with the UV irradiation increased to 66.2 mg m^{-3} after 75 min, which was 1.8 times larger than that produced at 240 °C without the UV irradiation. The average CO_2 formation rate in the photothermo-oxidation and thermo-oxidation of benzene at 240 °C in 75 min was calculated to be

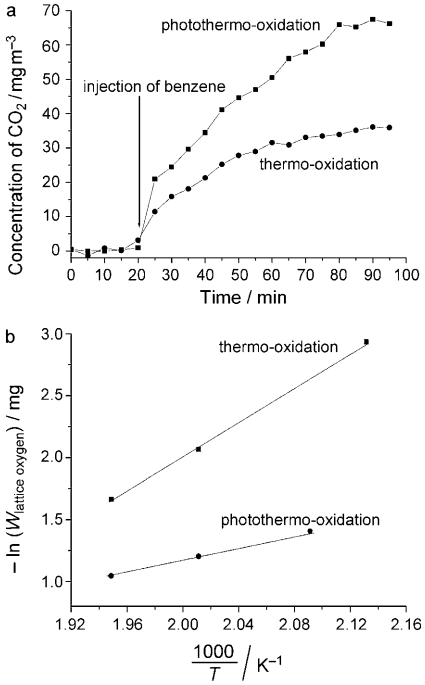

Figure 3. a) CO_2 concentration in the atmosphere of highly pure Ar after the injection of benzene (2 μL) into the reactor with the TiO_2 catalyst (0.5000 g) at 240 °C with or without UV irradiation as a function of time; b) an Arrhenius plot showing the temperature dependence of the consumed lattice oxygen for the photothermo-oxidation and thermo-oxidation reactions.

4.8×10^{-3} and 2.6×10^{-3} μmol g_{cat}^{-1} s^{-1}, respectively. Muggli et al. studied the photo-oxidation of formic acid by the lattice oxygen in TiO_2 (P25) in absence of O_2, and reported that upon UV illumination, the CO_2 formation rate quickly reached a maximum and then rapidly decreased; after 2200 s of photo-oxidation, the rate was approximately 8.0×10^{-3} μmol g_{cat}^{-1} s^{-1}, which was 8% of the initial rate.[18] The lower CO_2 formation rate in the photothermo-oxidation of benzene in our case than that in the photo-oxidation of formic acid was most probably due to the fact that benzene is chemically more stable than formic acid.

The corresponding $\ln(W_{\text{lattice oxygen}})$ versus T^{-1} plots ($W_{\text{lattice oxygen}}$ is the amount of consumed lattice oxygen) for both the thermo-oxidation and the photothermo-oxidation fit an Arrhenius-type behavior (Figure 3b). The apparent activation energy (E_a) calculated for the thermo-oxidation and the photothermo-oxidation was 58.1 and 21.1 kJ mol^{-1}, respectively. These results reveal that UV irradiation leads to a great decrease of the activation energy for the benzene oxidation by lattice oxygen, which account for the much higher efficiency for the photothermocatalytic oxidation than the thermocatalytic oxidation. The oxidation of benzene under the photothermocatalytic condition (in the atmosphere of air) at the different temperature was evaluated. The photothermocatalytic oxidation fit an Arrhenius-type behavior (Figure S5). Its E_a (20.7 kJ mol^{-1}) was almost equal to that of the photothermo-oxidation of benzene by the lattice oxygen. These results reveal that in the Mars–van Krevelen redox cycle, the oxidation

of benzene by the lattice oxygen in the TiO_2 catalyst plays an important role in the photothermocatalytic oxidation.

The benzene oxidation by the lattice oxygen was probed by in situ Raman spectra (Figure 4). TiO_2(P25) exhibited the strong bands at 143, 395, 513, and 637 cm^{-1}, which were attributed to the E_g, B_{1g}, A_{1g}, and E_g modes of anatase, respectively, and the small band at 450 cm^{-1} was assigned to the E_g mode of

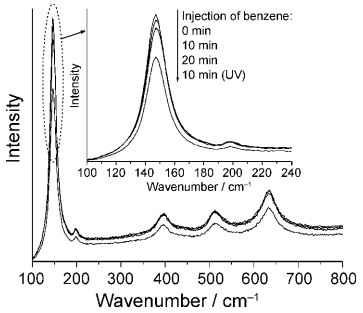

Figure 4. The Raman spectra of TiO_2 after the injection of benzene in the atmosphere of highly pure Ar with or without UV irradiation at 240 °C.

rutile.[19] The low-frequency modes at E_g of 144 cm^{-1} and at B_{1g} of 395 cm^{-1} are O–Ti–O bending type vibrations whereas the modes at E_g of 640 cm^{-1} and at A_{1g} are the Ti–O bond stretching type vibrations.[20] After the injection of benzene for 10 min without UV irradiation, there was a slight decrease in the Raman intensity of the O–Ti–O bending type vibration, suggesting a decrease in the amount of O–Ti–O bending type vibration in the TiO_2 sample due to the extraction of the lattice oxygen and thus the formation of oxygen vacancy (O–Ti–Ov–Ti–O) in TiO_2 caused by the thermo-oxidation. After 20 min, the decrease in the Raman intensity was enlarged, indicating that more lattice oxygen was consumed. It is interesting that after the UV irradiation for 10 min, the Raman intensity of O–Ti–O bending type vibration exhibited a considerable decrease. These results revealed that the photothermo-oxidation consumed much more lattice oxygen than the thermo-oxidation, which is in agreement with the above observation that the photothermocatalytic oxidation produces much more CO_2 than the thermocatalytic oxidation.

The high photothermocatalytic efficiency of TiO_2 can be further improved by the formation of Pt/TiO_2 nanocomposite, which can couple the excellent thermocatalytic function of Pt nanoparticles with the photothermocatalytic function of TiO_2. Well-dispersed Pt nanoparticles with small sizes on TiO_2 are very important for achieving a high activity of this catalyst for thermocatalytic and photocatalytic oxidation.[21] Here, such Pt/TiO_2 nanocomposite with a small Pt loading of 0.1 wt% was prepared by a novel method of gas-solid-phase photothermocatalytic reduction of H_2PtCl_6 adsorbed on TiO_2(P25) with ethanol as the scavenger of photogenerated holes (see the Experimental Section for details). Figure 5a shows the transmission electron microscopy (TEM) image of the 0.1 wt% Pt/TiO_2 catalyst. Pt nanoparticles with a narrow size distribution (1.8 to 3.2 nm; average particle size: 2.4 nm) were well dispersed on

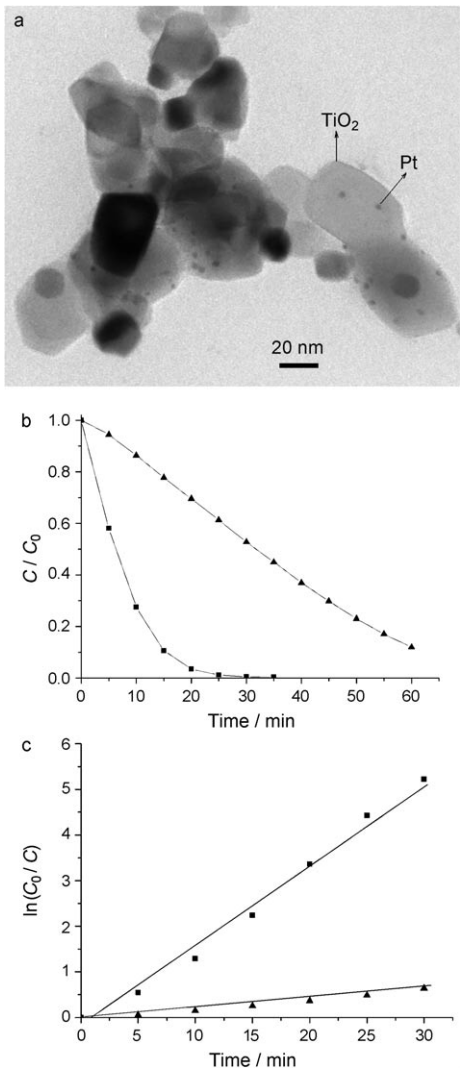

Figure 5. a) The TEM image of the 0.1 wt% Pt/TiO_2 catalyst; b) the time course of the decrease in the benzene concentration and c) $\ln(C_0/C)$ on the 0.1 wt% Pt/TiO2 catalyst under different conditions: photothermocatalytic oxidation with UV irradiation at 240 °C (■); thermocatalytic oxidation at 240 °C (▲).

the surface of the TiO_2 nanoparticles. The XRD profile of the Pt/TiO_2 catalyst (Figure S4) only shows the diffraction of TiO_2 and no characteristic Pt diffraction, further confirming the very small size of the Pt particles that are well dispersed on TiO_2.[21b] The Pt/TiO_2 catalyst has a specific surface area that is the same as the pure TiO_2 catalyst (56.0 $m^2 g^{-1}$). The conventional approach of preparing a Pt/TiO_2 photocatalyst by the photocatalytic reduction of H_2PtCl_6 under aqueous conditions usually led to the formation of larger Pt nanoparticles through a mechanism of cathodic-like reduction at small metallic nuclei or agglomeration of individual Pt atoms after a prolonged irradiation time.[22] Ikeda et al. reported a strategy for preparing well-dispersed Pt nanoparticles with an average size of 2.9 nm by preventing the nuclei growth and agglomeration through the photocatalytic reduction of H_2PtCl_6 and simultaneous deposition of phenolic polymers on the produced Pt nanoparticles by the photooxidation of phenol on TiO_2.[23] The present method

can avoid the nuclei growth and agglomeration due to the more efficient inhibition of the diffusion of $PtCl_6^{2-}$ ions and Pt^0 atoms in the gas-solid state than in the aqueous state, and thus, well-dispersed Pt nanoparticles were formed.

Compared with the pure TiO_2 catalyst, the 0.1 wt% Pt/TiO2 catalyst exhibited much enhanced photothermocatalytic activity for the oxidation of benzene (Figure 5b). Benzene was completely oxidized only after 30 min. No organic products were detected by GC besides CO_2. Its photothermocatalytic rate constant at 240 °C ($k_{ptc-Pt/TiO2} = 0.18\ min^{-1}$) was three times higher than that of the pure TiO_2 catalyst (Figure 5c). The Pt/TiO_2 catalyst exhibited an excellent durability for the photothermocatalytic oxidation evidenced by the observation that its photothermocatalytic activity remained unchanged even after it had been recycled 40 times (Figure S6). The Pt/TiO_2 electrode exhibited a photocurrent similar to that of the TiO_2 electrode at 240 °C (Figure 2), which implied that the Pt nanoparticles deposited on TiO_2 did not increase the separation of photogenerated electron–hole pairs in TiO_2, and increased the photocatalytic efficiency of TiO_2 at 240 °C. The dramatic enhancement may have originated from the excellent thermocatalytic activity of the supported Pt nanoparticles. Compared with the pure TiO_2 catalyst, the Pt/TiO_2 catalyst exhibited much enhanced thermocatalytic activity at 240 °C (Figure 5). Its thermocatalytic rate constant ($2.1 \times 10^{-2}\ min^{-1}$) was 11.7 times higher than that of the pure TiO_2 catalyst (Figure 1c and Figure 5c). This result indicated that the thermocatalytic efficiency of TiO_2 can be greatly enhanced by the surface modification of TiO_2 with Pt nanoparticles. The photothermocatalytic oxidation on the Pt/TiO_2 catalyst involves two processes as follows: the photothermocatalytic oxidation on TiO_2 and the thermocatalytic oxidation on supported Pt nanoparticles. If the two processes independently proceed, that is, $dC/dt = k_{ptc-TiO2}C + k_{tc-Pt}C$, then $k_{ptc-Pt/TiO2}$ should be equal to $k_{ptc-TiO2} + k_{tc-Pt}$ ($8.1 \times 10^{-2}\ min^{-1}$). However, $k_{ptc-Pt/TiO2}$ was 2.2 times higher than ($k_{ptc-TiO2} + k_{tc-Pt}$). Therefore, there was another synergetic effect between the photothermocatalytic oxidation on the TiO_2 particles and thermocatalytic oxidation on the supported Pt nanoparticles.

As discussed earlier, the catalytic oxidation of benzene on TiO_2 followed a Mars–van Krevelen redox mechanism: Benzene was first oxidized by the lattice oxygen in TiO_2 catalyst, and then the reduced TiO_{2-x} catalyst was reoxidized later by gaseous oxygen. On the Pt/TiO_2 catalyst, oxygen (O_2) dissociatively adsorbed onto the Pt nanoparticles to give surface O(Os) adatoms while oxygen adsorption over pure TiO_2 was molecular.[24] There was a spillover of the Os adatoms from Pt nanoparticles to the surface of the support (e.g.,TiO_2).[25,26] Under the thermocatalytic condition, the spillover Os adatoms oxidized benzene and the reduced TiO_x catalyst to CO_2 and TiO_2, respectively, which resulted in the efficient thermocatalytic oxidation of benzene. Under the photothermocatalytic conditions, UV irradiation greatly accelerated the oxidation of benzene by the lattice oxygen in the TiO_2 catalyst whereas the spillover Os adatoms from Pt nanoparticles greatly accelerated the reoxidation of the reduced TiO_x catalyst as the Os adatoms were much more active than gaseous O_2. Thus, the Mars–van Krevelen redox cycle was synergetically accelerated, which resulted in the excellent photothermocatalytic activity of the Pt/TiO_2 nanocomposite.

In summary, the high efficient photothermocatalytic oxidation of benzene has been realized by coating TiO_2 sample on the surfaces of a UV lamp without using any additional heater, which makes the TiO_2 catalyst co-excited by both UV irradiation and thermal energy. The much higher efficiency of the photothermocatalytic oxidation than the combination of both photocatalytic and thermocatalytic oxidation of benzene is attributed to the existence of a photothermocatalytic synergetic effect, which greatly decreases the activation energy of benzene oxidation by the lattice oxygen in TiO_2. The high photothermocatalytic efficiency of TiO_2 can be significantly enhanced by the surface modification of TiO_2 with a small amount of well-dispersed Pt nanoparticles due to the synergetic effect of oxygen spillover from Pt nanoparticles. Such low loading of noble metal Pt (e.g., 0.1 wt%) does not increase the cost of the catalysts. The present findings are easily applicable to various photocatalytic materials, and thus may lead to a general strategy of developing long-term efficient and cost-effective catalytic detoxification of air organic pollutants.

Experimental Section

Materials: Titania P25 (TiO_2, ca. 80% anatase, 20% rutile) was purchased from Deggussa Co. $H_2PtCl_6{\cdot}6H_2O$, benzene, ethanol, and poly(ethylene glycol) were purchased from Shanghai Chemical Co.

Characterization: Fourier transform infrared (FTIR) spectra were taken on a Thermo Nicolet Nexus spectrometer. The catalyst sample was analyzed by an ESCALab MK2 X-ray photoelectron spectrometer using Mg Kα radiation. The XRD patterns were obtained on a Rigaku Dmax X-ray diffractometer using Cu Kα radiation. The TEM images were obtained by using a JEM-100CX electron microscope. The BET surface area was measured on AUTOSDRB-1 using N_2 adsorption at −196 °C for the sample predegassed at 200 °C in vacuum for 2 h. In situ Raman spectra were recorded on a Renishaw inVia Raman microscope equipped with a hot–cold cell (THMS600) using an excitation of 514.5 nm laser light. A 125 W self-rectified high pressure Hg lamp (Shanghai Yaming Lighting Appliance Co., denoted as UV lamp) was used as a light source. The TiO_2 sample was set on the sample stage of the cell, and heated to different temperatures. Benzene (2 μL) was injected into the cell after the cell was purged with highly pure Ar.

Photocurrent measurements: A mixture of TiO_2 powder and poly(ethylene glycol) with a weight ratio of 5% was added to ethanol (15 mL), and ultrasonicated for 30 min. The obtained mixture was uniformly spread on an indium tin oxide (ITO) glass substrate (1 cm × 1.2 cm). Another ITO glass substrate was covered on the mixture to form an ITO/film/ITO stack. After the evaporation of ethanol, the sample was heated to 480 °C in a muffle furnace at a rate of 2 °C min^{-1}, and remained at this temperature for 6 h to completely remove poly(ethylene glycol). The electrical lead of Au fine wire (Ø 0.05 mm) was attached to the ITO electrodes by using Au paste. The transient response of photocurrent for the TiO_2 electrode under the irradiation of an UV lamp at a different temperature was recorded under an operation voltage of 0.5 V on an electrochemical analyzer (CHI750). The temperature was controlled by a hot plate(C-MAG HP-7).

Catalytic activity: The catalytic activity of the TiO_2 catalyst for the gas-phase oxidation of benzene was tested on a closed cylindrical stainless gas-phase batch reactor with a volume of 7.2 L. An UV lamp was set on the inner wall of the reactor. The reactor was connected to a GC 9560 gas chromatograph equipped with a flame ionization detector (FID), a methane converter, a Porapak R column and PEG20M column through an automatically sampling ten-way valve (VALCO) with an air actuator. TiO_2 powder (0.5000 g) was added to ethanol (40 mL) and ultrasonicated for 2 h. The TiO_2 suspension was coated on the UV lamp, and dried under an infrared lamp. The specific amount of TiO_2 on the UV lamp was 2.1×10^{-3} g cm^{-2}. After a known amount of benzene (2 μL) was injected in the reactor, the UV lamp was turned on. The concentration of CO_2 produced was obtained by subtracting the initial concentration of CO_2 in air. For testing the thermocatalytic and photocatalytic oxidation of benzene, TiO_2 powder (0.5000 g) was dispersed on a glass dish, and set on the bottom of the reactor. The reactor was put on a heating plate to control the reaction temperature without UV irradiation. For testing the photocatalytic oxidation, the reactor was put in an ice-water bath to maintain the reaction temperature at 40 °C under the irradiation of the UV lamp. The intensity of the UV light in the region of 320–400 nm emitted from the UV lamp, of which maximum UV irradiation was centered at 365 nm, was measured with an UV-A radiometer. The procedure for the recycled experiments of the TiO_2 catalyst is as follows: After the first catalytic activity test, the reactor was opened to remove the products (e.g., CO_2) with fresh air and then covered again. Then, benzene (2 μL) was injected in the reactor, and the lamp was turned on to start the next test of catalytic oxidation. These cycles were repeated 40 times.

Preparation of Pt/TiO_2 catalyst: TiO_2 powder (0.5000 g) was added to distilled water (20 mL) in a beaker and ultrasonicated for 2 h. H_2PtCl_6 aqueous solution (0.16 wt%, 0.66 mL) was added to the TiO_2 suspension under magnetic stirring. The mixture was coated on an UV lamp, and dried under an infrared lamp. The UV lamp covered by a coating of H_2PtCl_6/TiO_2 nanopowder was set on the inner wall of the reactor, and aqueous ethanol solution (10 vol%, 20 mL) in a beaker was placed on the bottom of the reactor. The UV lamp was turned on after the reactor was closed. The ethanol aqueous solution was evaporated by thermal energy emitted from the UV lamp. The H_2PtCl_6 supported on TiO_2 was irradiated for 3 h and photothermocatalytically reduced by gaseous ethanol to Pt nanoparticles.

Acknowledgements

This work was supported by National Basic Research Program of China (2009CB939704), Important Project of Ministry of Education of China (309021), Scientific Research Foundation for the Returned Overseas Chinese Scholars ([2008] 890), and Nippon Sheet Glass Foundation.

Keywords: heterogeneous catalysis · nanoparticles · photocatalysis · platinum · supported catalysts

[1] H. L. Chen, H. M. Lee, S. H. Chen, M. B. Chang, S. J. Yu, S. N. Li, *Environ. Sci. Technol.* **2009**, *43*, 2216.
[2] X. N. Zhang, J. H. Huang, K. N. Ding, Y. D. Hou, X. C. Wang, X. Z. Fu, *Environ. Sci. Technol.* **2009**, *43*, 4164.
[3] R. Méndez-Román, N. Cardona-Martínez, *Catal. Today* **1998**, *40*, 353.
[4] W. Wu, L. Liao, C. Lien, J. Lin, *Phys. Chem. Chem. Phys.* **2001**, *3*, 4456.
[5] a) H. Einaga, S. Futamura, T. Ibusuki, *Environ. Sci. Technol.* **2001**, *35*, 1880; b) H. Einaga, S. Futamura, T. Ibusuki, *Environ. Sci. Technol.* **2004**, *38*, 285.
[6] Y. L. Chen, D. Z. Li, X. C. Wang, X. X. Wang, X. Z. Fu, *Chem. Commun.* **2004**, 2304.
[7] C. J. Ren, T. Zou, G. Q. Chen, Y. Q. Chen, M. C. Gong, *Chin. J. Catal.* **2006**, *27*, 1048.
[8] K. P. Yu, G. W. M. Lee, *Appl. Catal. B* **2007**, *75*, 29.
[9] J. Jeong, K. Sekiguchi, W. Lee, K. Sakamoto, *J. Photochem. Photobiol. A* **2005**, *169*, 279.
[10] a) B. Y. Lee, S. H. Park, S. C. Lee, M. Kang, S. J. Choung, *Catal. Today* **2004**, *93*, 769; b) T. Sano, N. Negishi, E. Sakai, S. Matsuzawa, *J. Mol. Catal. A: Chem.* **2006**, *245*, 235.
[11] D. C. Eaton, *Laboratory Investigation in Organic Chemistry*, McGraw-Hill, NY, **1989**.
[12] a) J. Zhou, S. Dag, S. D. Senanayake, B. C. Hathorn, S. V. Kalinin, V. Meunier, D. R. Mullins, S. H. Overbury, A. P. Baddorf, *Phys. Rev. B* **2006**, *74*, 125318; b) H. Raza, P. L. Wincott, G. Thornton, R. Casanova, A. Rodriguez, *Surf. Sci.* **1998**, *402–404*, 710.
[13] T. Bak, J. Nowotny, M. Rekas, C. C. Sorrell, *J. Phys. Chem. Solids* **2003**, *64*, 1069.
[14] G. C. Bond, *Heterogeneous Catalysis: Principles and Applications*, 2nd ed., Clarendon Press, Oxford, **1987**.
[15] I. E. Wachs, J. M. Jehng, W. Ueda, *J. Phys. Chem. B* **2005**, *109*, 2275.
[16] D. A. Panayotov, J. R. Morris, *J. Phys. Chem. C* **2009**, *113*, 15684.
[17] T. L. Thompson, D. A. Panayotov, J. T. Yates Jr. , *J. Phys. Chem.B* **2004**, *108*, 16825.
[18] D. S. Muggli, J. L. Falconer, *J. Catal.* **2000**, *191*, 318.
[19] Y. H. Zhang, S. G. Ebbinghaus, A. Weidenkaff, T. Kurz, H. A. K. von Nidda, P. J. Klar, M. Gungerich, A. Reller, *Chem. Mater.* **2003**, *15*, 4028.
[20] T. Takahashi, H. Nakabayashi, J. Tanabe, N. Yamada, *J. Vac. Sci. Technol. A* **2003**, *21*, 1419.
[21] a) C. B. Zhang, H. He, K. Tanaka, *Appl. Catal. B* **2006**, *65*, 37; b) Y. Xie, K. L. Ding, Z. M. Liu, R. T. Tao, Z. Y. Sun, H. Y. Zhang, G. M. An, *J. Am. Chem. Soc.* **2009**, *131*, 6648.
[22] J. M. Herrmann, J. Disdier, P. Pichat, *J. Phys. Chem.* **1986**, *90*, 6028.
[23] Y. H. Ng, S. Ikeda, T. Harada, S. Higashida, T. Sakata, H. Mori, M. Matsumura, *Adv. Mater.* **2007**, *19*, 597.
[24] D. Uner, N. A. Tapan, I. Ozen, M. Uner, *Appl. Catal. A* **2003**, *251*, 225.
[25] F. Donga, A. Suda, T. Tanabe, Y. Nagai, H. Sobukawa, H. Shinjoh, M. Sugiura, C. Descorme , D. Duprez, *Catal. Today* **2004**, *90*, 223.
[26] H. X. Lin, *J. Mol. Catal. A: Chem.* **1999**, *144*, 189.

Received: March 23, 2010
Published online on June 10, 2010

